Erasmus Mundus Master in Membrane Engineering

2011-2013

4th semester

Membrane Filtration for wastewater treatment applications

Papoutsoglou Dimitra
Project supervisor: prof. Chris. Paraskeva
Module supervisor: prof. Reyes Mallada

Patras, July 2013

The EM3E Master is an Education Programme supported by the European Commission, the European Membrane Society (EMS), the European Membrane House (EMH), and a large international network of industrial companies, research centres and universities

Visit EM3E internet site: *www.em3e*

The EM3E education programme has been funded with support from the European Commission. This publication reflects the views only of the author, and the Commission cannot be held responsible for any use which may be made of the information contained therein.

1. Contents

Index of Figures

Index of Tables

Prologue

I well over remember the moment when my application to the EM3E was accepted and EM3E master committee announced a favourably advise on it. Since two years, me and all my colleagues did experienced an offspring program becoming reality and membrane engineering is ending to give finally its first alumni.

Working on my master thesis, I mainly worked on dye industry wastewater treatment with conventional methods and membrane processes. We handled several unexpected difficult tasks mainly on membranes embedded with carbon nanotubes, a quite innovative field. In this manuscript, successful experiments and conclusions are reported. The subject raises high expectations and I conclude that it should steadily get across lab scale to large scale applications.

I am grateful to professors Christakis Paraskeva, George Voyiatzis and Reyes Mallada who offered me the opportunity making my project on this subject and undoubtedly to all the people involved to my project, especially phD candidates of Patras University, Giannis Anastasopoulos, Spyros Kontos, Zagklis Dimitris, Eleni Moschopoulou. My warmer acknowledgements also are addressed to my EM3E colleagues, all my professors and master organizers and secretaries. Last, but not least, both my family and my husband who stand by me during Erasmus experience. This is the line dropped to express my gratitude to them.

Abstract

Membranes are used for particles or molecules separation in plethora processes of extraction, adsorption and filtration for liquid-liquid, gas-liquid, gas-solid, liquid-solid or gas-gas separation. In sector of wastewater works, membranes are already commercial applied for reverse osmosis, ultrafiltration, nanofiltration and bioreactors. Crucial drawbacks in membrane filtration technology are both irreversible fouling of membranes and high energy dissipation usually applied for pressure drop. Innovative membranes with embedded carbon nanotubes can be an optimal solution to overpass these drawbacks.

In industry, the first water treatment involves processes of a purely physical, mechanical and chemical nature to reduce the solid content. The technological evolution has led to

widespread mechanisation of the systems. The quality of water supplies has gradually declined largely because of excessive consumption of natural water and the abuse of ground soil as a recipient of wastewater. Pollution has also contributed to this effect. An existing physicochemical treatment is tried to be optimized controlling different parameters of sedimentation part and raw materials use. Wastewater from the industry is collected and characterised. The first batch is treated using a coagulation-flocculation process to remove large particles remaining in the sludge (primary treatment). The product is completely separated in supernatant solution and sludge. Supernatant is sampling for different flocculants concentration. A new polyelectrolyte (PDADMAC) is tested in terms of alkalinity and the results are compared with current electrolyte (PAC). All samples before and after the process are characterised using zeta size and particle size measurements together with COD and total solids measurements. The supernatant from primary treatment process is fed to ultrafiltration unit (UF) (secondary treatment). The permeate outlet from UF is fed to nanofiltration (NF) where almost all organics and solids are removed. The final NF permeate shows very high purity containing only mono and divalent ions of salts. A tertiary treatment refines the water product of nanofiltration membranes using commercial polymeric membranes with embedded aligned carbon nanotubes (CNTs). Before applying the hybrid membranes a full detailed study has been carried out in terms of CNTs embedment, water and wastewater flux permeability and SEM microscopy. Polymeric membranes embedded with CNTs have been made in the laboratory with spin coating method and by ultrafiltration unit size exclusion is tested using PEG solutions.

Nomenclature

DWCNTs	Double Walled Carbon Nanotubes
CNTs	Carbon Nanotubes
CVD	Carbon Vapor Deposition
GPC	Gel Permeation Chromatography
MD	Monte Carlo Simulation
MTWW	Model Textile Waste Water
MWCO	Molecular Weight Cut Off
PAC	Poly(aluminum chloride)

PDADMAC	Poly(diallyldimethylammonium chloride)
PEG	Polyethylene glycol
SDS	Sodium Dodecyl Sulfate
TS	Total Solids

PART A: Dye industry wastewater treatment

1. Theoretical background

1.1 Paint industry wastewater

The main sources of wastewater in dye industry are tanks of dye solution (baths), reflux water, washing water and run-off rain water. In the current work, treated waste is mainly the washing waters of the polymerization tanks and contains the products of the industry diluted, which are polyvinyl acetate and poly(acrylic esters). The concentration of pollutants can widely vary and quantities generally differ also depending on the batch. The different sorts of pollutants can be divided in organic, inorganic molecules and metal ions. Some compounds are highly toxic and mutagenic and many studies have shown relation between this kind of wastes and carcinogenic amines (1), (2). The presence of residual chemicals is strongly undesirable especially if wastewater is disposed in natural sources due to depletion of the dissolved oxygen. Dye industry wastewater can contain impurities, dispersed solids, additives such as sodium chloride, sodium carbonate, sulphate cellulose etc changing in batch mode. Organic molecules containing in the dye wastewater can be chromophore, auxochrome and also heavy metals as chromium, lead, iron, aluminium. In common practice, it is not a matter of only one step dye wastes purification and more than two steps are usually used (2).

1.2 Coagulation – Flocculation

Coagulation is the destabilization of solution via minimizing zeta potential. Coagulants can be classified into two main categories: metal coagulants and polymers. Flocculation is the process of whereby destabilized particles from larger agglomerates due to surficial tendencies (2). Both practices are well known since hundreds of years (4). In dye industry

coagulation/flocculation offers a low cost treatment method and several coagulants/flocculants are applied (see Table 1).

Table 1 Dye removal using inorganic coagulants with organic polymers as flocculant aids (2)

Type of dyes	Inorganic coagulants	Type of polymer	Condition	Performance
Real textile wastewater	Aluminium based (2g/l)	Cationic polymer – Cyanoguanidine – formaldehyde (500mg/L)	Final pH: 5 40^{o}C Mixing time =11min Settling time = 30min	Colour removal=60% Turbidity removal =80% COD removal= 28%
100mg/L reactive blue STE	Polyferric chloride	Cationic (polyDADMAC*) (dosage of composite=20mg/L)	Initial pH:7 Ambient temperature Mixing time=15min Settling time=12min	Colour removal=90%
Real wastewater from fabric dyeing industry	Aluminium oxide, Al_2O_3 (1800mg/L)	Cationic (polyDADMAC) (dosage of composite=30mg/L)	Initial pH:5.7-5.9 Ambient temperature Mixing time=11min Settling time=30min	Colour removal=69% Turbidity removal =99%

Optimization of coagulation/flocculation process is an intriguing target given that industrial dyes prove high water solubility and consist of complex usually not well known substances. All the methods and systems must be designed for large scale applications. Many references show large differences above ferrous or aluminium flocculants. Aboulhassan et al. (5) have achieved a COD reduction of 91% with the use of $FeCl_3$ combined with high molecular weight polyelectrolytes (flocculants). Other coagulants like $FeSO_4$, $Al_2(SO)_4$, and

poly(aluminum) chloride have been used in combination with high molecular weight polymers, yielding high COD reduction.

1.3 Polyelectrolytes

The first polyelectrolyte that is used is poly(aluminum chloride) (commercial named PAC) and anionic poly -(acrylamide) that are supplied by the physicochemical treatment routinely applied at the industrial plant. The new polyelectrolyte that also used is poly(diallyldimethylammonium chloride) (PDADMAC) with average M_w<100000, 35wt% in H_2O, CAS 26062-79-3, supplied by Sigma Aldrich.

2. Experimental procedure

2.1 Characterization of wastewater

In all cases pH, particle size, organic load and ζ potential values of the raw materials are measured before the decision of the appropriate treatment. The products of studied plant are alkyd and acrylic resins, unsaturated polyester resins and resins for powder coatings, and PVA homopolymers & copolymers. The initial organic load of wastewater is given as COD 20.000-30.000mg/L, residual of raw compound as monomers, polyacrylic esters and others. Alkalinity of dye wastewater is slightly basic of pH 5.5-7. For the conducted experiments, four samples (sample 1, 2, 3 4) of wastewater are used taken from the equalization tank of the industry.

Table 2 Properties of Wastewater Samples

Parameter	1st sample	2ond sample	3rd sample	4th sample
COD (mg/L)	16710±280	19887±70	960±212	22167±462
TS (g/l)	11.5±0.01	10.21±0.61	5.64±0.08	9.65±0.21
ζ potential (mV) mean values	-1.02	-30.7	-2.52	-29.6
Particle size (nm) mean values	3797 (82%) 285 (18%)	187 (100%)	83 (100%)	200.9

Sample 1st, 2ond and 4th are treated with the coagulation/flocculation process, while the third one is tested in membrane system. Sample 3rd is coming from existing treatment plant of industry with 1000mg/l PAC and flocculant.

2.2 Coagulation/Flocculation

The coagulation/flocculation experiments are carried out in a jar test apparatus, with six beakers of 1 L in volume. Initially a sample of waste is placed in each beaker, and their pH is adjusted with solutions of NaOH and HCl. Solubility of aluminium hydroxide increases in basic pH values and PAC gives better results in this area. The initial pH is near 6 and is increased to 12 for most of the coagulation experiments, except for the group of experiments for the optimization of pH in PDADMAC case, where it is set from 3 to 12.

In next step, coagulant is added and rapid mixing for 3 min makes ζ potential destabilization and then agglomeration process. Waste is then homogenised and suspended particles are neutralized. In case of flocculant addition, mixing goes for more 10 min where further agglomeration of formed flocs takes place (4). In the experiments that no flocculant is used, the step of slow mixing is preserved. The waste is finally left for its sedimentation and after two hours, samples are collected by supernatant phase for measurements.

The first treatment step is the implementation of different polyelectrolytes for the coagulation of the wastewater and the definition of the optimum treatment conditions. The target of dye wastewater treatment is the reuse of final product in the production line of the company. According to the literature, the reuse standards are gathered in Table 3:

Table 3 General requirement for reused water (2)

Parameter	Textile	Carpet industry
COD (mg/L)	60-80	8-40
Conductivity (μS/cm)	1000	-
pH	6-8	-
Turbidity (NTU)	1	15
Colour (Pt-Co)	None	0-20
Suspended solids (mg/L)	5	-
Dissolved solids (mg/L)	500	500
Total hardness (mg/L as $CaCo_3$)	25-50	60

2.3 PAC optimization

The first step of the present work is the optimization of the existing process, in terms of coagulant/flocculant dosage and pH. The coagulant used is poly (aluminium chloride) (PAC), and anionic poly-(acrylamide) is used as flocculant, at pH 12. In the current physicochemical treatment of the industry, coagulation/flocculation method is applied using polyaluminium chloride (PAC) as coagulant and polyvinylochloride as flocculant. The concentration is 1000mg/L of PAC and unknown value of flocculant. The final effluent of the industry is 100m^3/day.

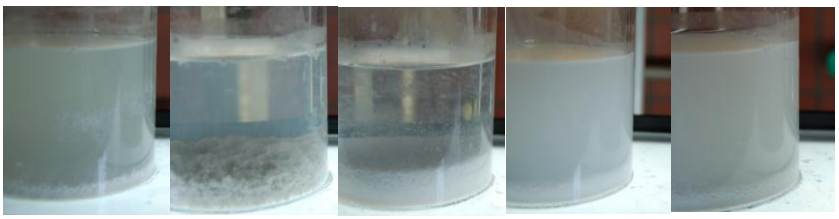

Figure 1 Jar test samples varying PAC concentration, sedimentation (PAC varying flocculant 10 mg/L, 2h, pH 12)

The first set of experiments is performed for constant pH 12 and flocculant dosage 10 mg/L (pH and flocculant concentration as suggested by industry). Polyecelectrolyte concentration (PAC) varied from 1 to 956mg/L (Table 4).

Table 4 Experimental Conditions for PAC optimization

PAC optimization		
Flocculant dosage(mg/L)	Coagulant dosage (mg/L)	pH
10	1	12
10	192	12
10	384	12
10	766	12
10	956	12

Figure 2 illustrates the variation of ζ potential, COD, and TS with polyelectrolyte (PAC) concentration. It is apparent that ζ potential is near zero at a coagulant dosage of 427 mg/L, and at the same area high reduction of COD and TS is obtained.

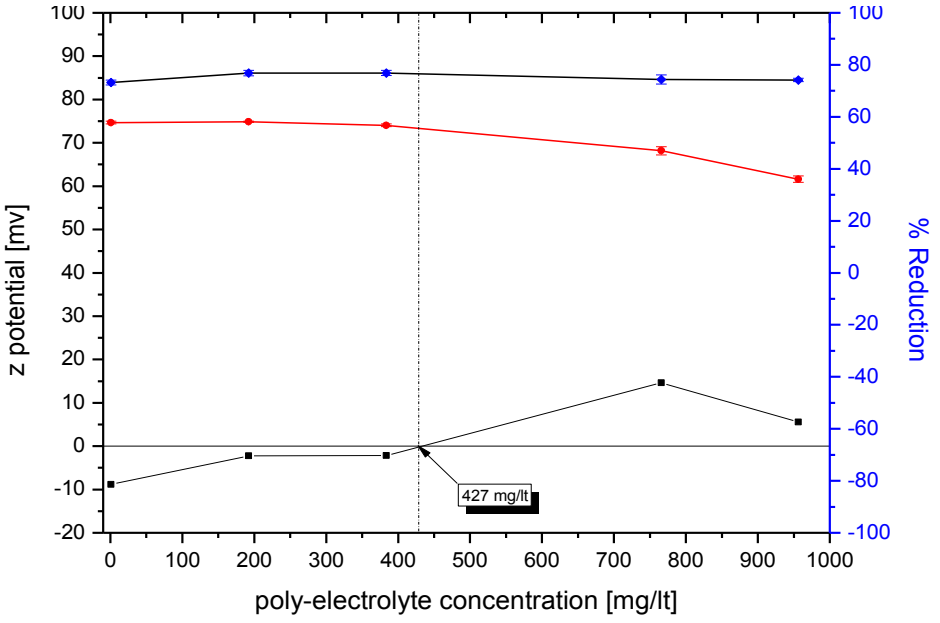

Figure 2 ζ-potential, COD and TS variation in function of polyelectrolyte concentration (PAC varying flocculant 10 mg/L, 2h, pH 12)

2.4 PDADMAC optimization

After the optimization of the existing treatment process, new polyelectrolyte is examined. The purpose is the replacement of PAC and anionic poly(acrylamide) with one polyelectrolyte that plays the role of both coagulant and flocculant at the same time. Also the possibility of higher COD and TS reduction is examined. The experiments with PDADMAC are carried out with Sample 4. PDADMAC is an organic polymer with cationic behaviour and it is because of that its encapsulating properties. It is product of dimethyldiathyl-ammonium chloride polymerization (p-DADMAC). High molecular mass of $3*10^6$Da enhances more coagulation and flocculation mechanisms. CAS name is 2-Propen-1-aminium, N, N-dimethyl-N-Propenyl-, chloride homopolymer and CAS number is 26062-79-3 and molecular formula $(C_8H_{16}NCL)n$, other commercial names can also be PDMDAAC.

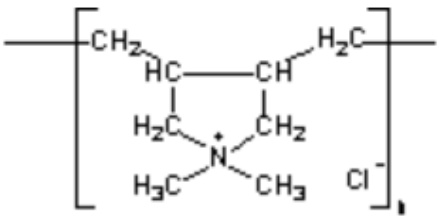

Figure 3 Structure formula of poly (dimethyl diallyl ammonium chloride) (6)

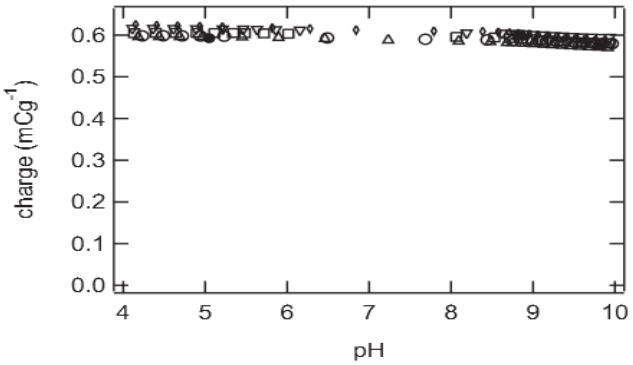

Figure 4 Proton binding isotherms of PDADMAC at five different ionic strengths: ○ 0.01M □ 0.05M △ 0.10M ▽0.5M ◊1.00M (6)

In the first batch of experiments, PDADMAC is tested at suggested pH value (12). The results (Table 5) verifies that at basic environment enhances electrolyte performance. Even though pH 12 is said to be optimal, proton binding isotherm (Figure 4) express charge of polyelectrolyte in function of pH. As it is illustrated in Figure 4, charge is independent of pH for different solutions. Hence, it is decided to control pH effect in PDADMAC efficiency. The summary table of the experiments are displayed below.

Table 5 Summary of experiments for PDADMAC optimization in function of pH

Parameter	Initial solution	pH 3	pH 6	pH 8	pH 10	pH 12
COD [mg/L]	22167±462	22892±605	7054±225	2157±42	1379±46	1295±56
TS [g/l]	9.65±0.21	6.55±1.20	0.65±0.92	0.6±0.14	0.95±0.07	2.3
Particle size [nm] mean value	200.9	223.9 (95.7%) 4660 (4.3%)	824.3 (65.5%) 196.3 (34.5%)	122.9	376.5	356.3
z-potential [mV]	-29.6±17.4	8.61±9.69	9.37±5.04	4.4±3.82	-1.52±4	-5.57±7.75

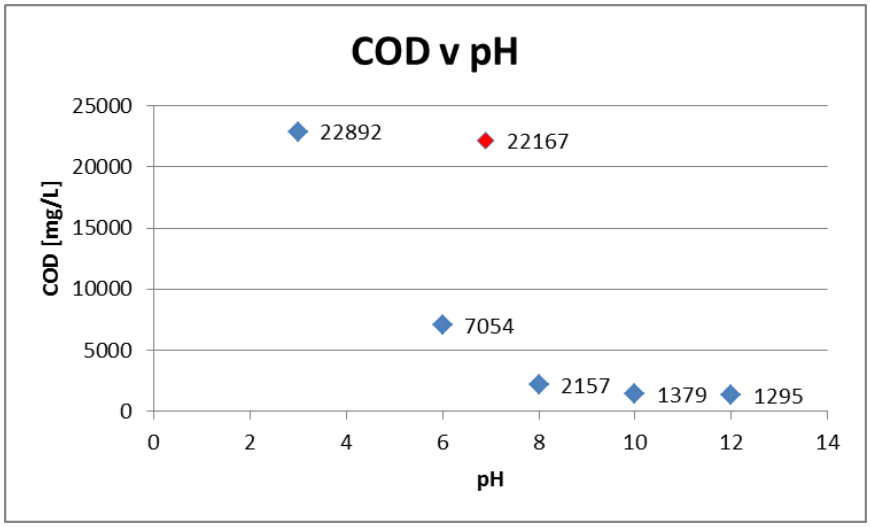

Figure 5 COD in function of pH for PDADMAC optimization experiments (500mg/L PDADMAC, 2h sedimentation, and varying pH)

In acid environment, polymeric electrolyte is not activated at all and both pH 3 and 6 give organic load values, 22892mg/L and 7054mg/L, definitely inappropriate towards reuse or disposal.

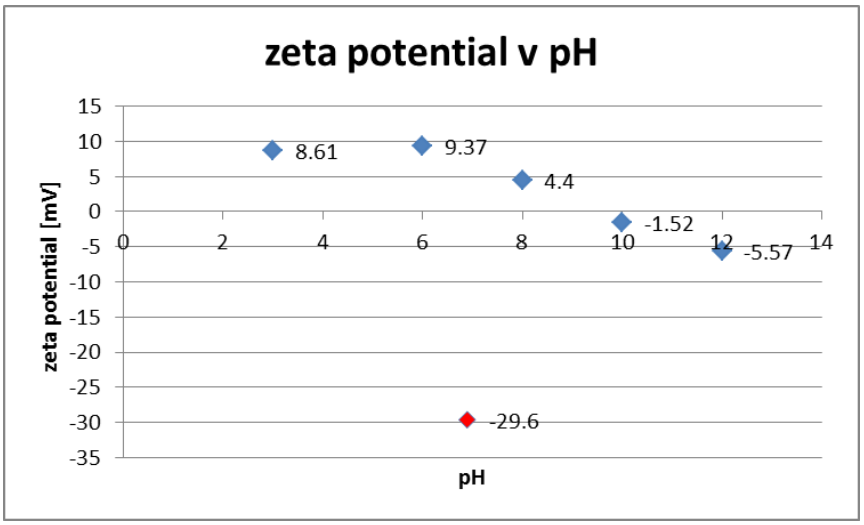

Figure 6 ζ-potential in function of pH for PDADMAC optimization experiments (500mg/L PDADMAC, 2h sedimentation, varying pH)

Total solids for pH 10 are 0.5g/L when for pH 12 are 2.3g/L and ζ-potential shows also lower for pH 10 than pH 12.

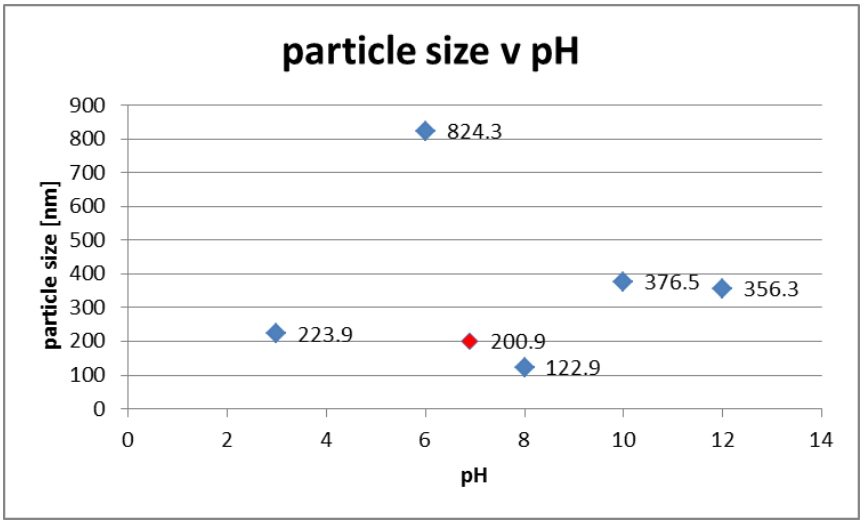

Figure 7 Particle size in function of pH for PDADMAC optimization experiments (500mg/L PDADMAC, 2h sedimentation, varying pH)

In pH 6, particle size even increased to 824.3 nm. For pH, COD is still high (2157 mg/L) when TS decrease to 0.6mg/L and particle size is relatively well control (122.9nm). Interest is pointed to higher pH values, 10 and 12 where PDADMAC works in the industry. For pH 10, COD is 1370 mg/L slightly higher than 1295mg/L for pH 12. Particle size cannot be taken into account given that for both pH are measured higher than initial solution particle size (376.5nm and 356.3nm respectively) probably made by electrolyte molecules.

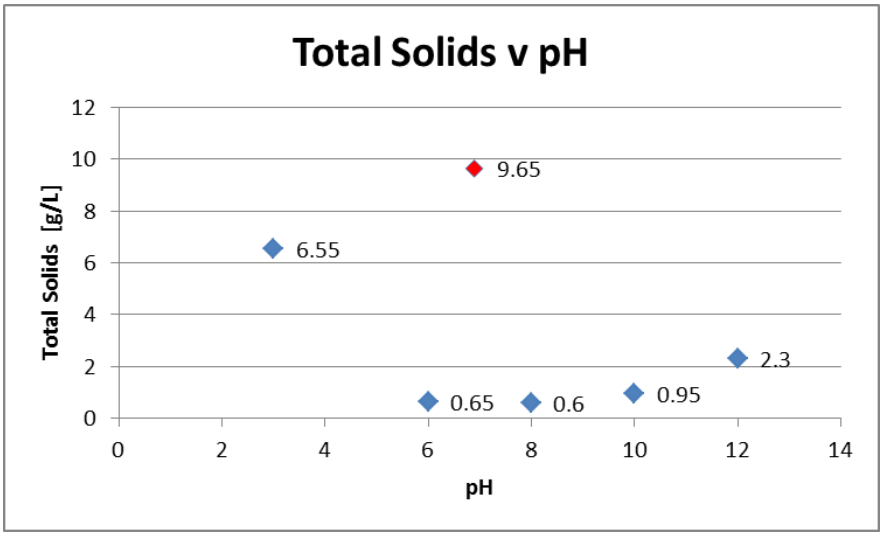

Figure 8 Total solids size in function of pH for PDADMAC optimization experiments (500mg/L PDADMAC, 2h sedimentation, varying pH)

Results regarding to total solids and particle size cannot be totally trustable and organic load need to be the main benchmarking for electrolyte evaluation.

In case of tertiary waste treatment, pH 10 can be a balanced choice requiring smaller amount of NaOH and saving chemicals in industrial scale applications.

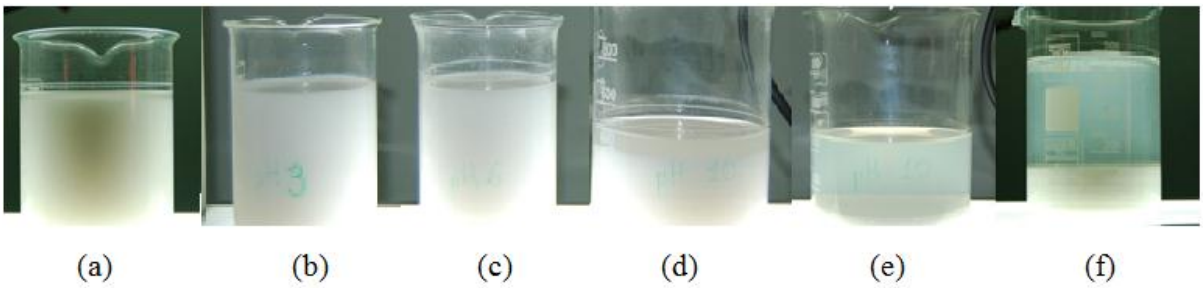

Figure 9 Dye industry wastewater (sample 3) treated with 500mg/L PDADMAC, stirring and after 2 hours of sedimentation

Comparing PDADMAC and PAC results, polymeric polyelectrolyte and metal coagulant, organic load decrease 94% for PDADMAC instead of 80% for PAC coagulant, ζ potential is significantly destabilized for both cases. Particle size is, though, higher for PDADMAC case (356nm) than 187nm for PAC because of larger organic agglomerates and high molecular size of polymeric electrolyte. Total solids appear less for PDADMAC (2.3g/l) than PAC case (4.7g/l). In overview, polymeric electrolyte gives better results for wastewater purification via coagulation/flocculation process.

2.5 Membrane Filtration

In literature, review paper present in abundance successful use of nanofiltration membranes in textile industry (1). Organic load and total solids can readily be removed by membrane modules given that waste is primary treated by coagulation/flocculation systems. The final target of a tertiary treatment as filtration membranes usually is related to recycling or disposal of the effluent. Organic load might differ from 30 to 100 mg/L and thus coagulation flocculation process does not fulfil disposal and reuse requirements (7). In next paragraphs, the results of membrane filtration are described. The pilotic systems are illustrated in the image below. The inlet of membrane step is provided by industrial wastewater treatment method.

2.6 Ultrafiltration

Initially the waste (sample 3), which is the final effluent of the existing physicochemical treatment process of the industry with the use of poly(aluminium chloride) and anionic poly(acrylamide), is treated with an ultrafiltration unit, in different transmembrane pressures (TMP) from 2.5 to 4 bar. Concentration of total solids is about 5 mg/L, and the mean particle size is close to 80 nm thanks to the efficient coagulation/flocculation process that is preceded.

Figure 10 Image Laboratory ultrafiltration unit

UF (Figure 10 **Image Laboratory ultrafiltration unit**) is implemented only to play an auxiliary role before the use of a more effective membrane (NF or RO). Because the mean size of suspended particles is 80 nm, and the mean pore of UF membrane modulus is 100 nm, TS reduction is practically zero and only particles with size larger than 100 nm are removed. However, UF led to the removal of 20% of the organic matter. An unpleasant result is that the flux that is acquired is low for an ultrafiltration process, which might have been caused by clogging of membrane pores by the suspended polymers. A high flux rate is recovered

after a thorough cleaning of the membranes with a NaOH solution for half an hour (85% of the initial flux rate).

Table 6 Experimental conditions and results for ultrafiltration

Parameter	Initial solution	Transmembrane pressure (ΔP) in filtrated solution			
		2.5 bar	3 bar	3.5 bar	4 bar
COD mg/L	950 ±17.3	818 ±15	765 ±55	828 ±10.8	792 ±148
T.S. g/l	4.93 ±0.07	4.82 ±0.28	5.18 ±0.08	5.14 ±0.23	5.04 ±0.06

2.7 Reverse Osmosis

The permeate stream of ultrafiltration is fed to a reverse osmosis unit. The results are very encouraging with COD and TS reduction being around 90−100%. Initial COD values at 960 mg/L are reduced to 16 mg/L after treatment with the RO process. TS is reduced dramatically and their value in permeate stream do not exceeded the value of 0.5 mg/L. On the other hand, irreversible fouling phenomena are observed, as the flux of clear water is not the same before and after the treatment of the waste, even after chemical cleaning of the membrane module. Implementation of membranes shall take place after a complete evaluation of all operational parameter values and of the problems related to their performance (flux decline, cleaning procedure, long-term behavior, etc).

Figure 11 Laboratory reverse osmosis unit

Table 7 Experimental conditions and results for reverse osmosis filtration

Parameter	Initial Solution	Transmembrane pressure in filtrated solution (bar)			
		10 bar	20 bar	30 bar	40 bar
COD mg/L	792±148	16±25	76±34	83±32	43±21
T.S. g/L	5.04±0.06	-0.09±0.07	0.23±0.04	0.39±0.18	0.42±0.25

2.8 Conclusions of Part A

Through a parametric study, the optimization of the existing physicochemical treatment process of a paint industry has been carried out, in terms of coagulant concentration and pH. In the first set of experiments, the coagulants and flocculants implemented are the ones that are currently in use in the wastewater treatment unit of the factory. It is found that higher removal efficiency could be achieved if lower concentration, compared to the one used by the industry, of polyelectrolytes is used (400 mg/L instead of 1000 mg/L). By working at higher concentrations of positive polyelectrolytes the negative ζ potential value of suspended particles is inverted to positive, stabilizing again the solution and the particles

remained under suspension. It is proved that the coagulant, if used in excess, can have negative effects on the separation. Moreover, a new polyelectrolyte that can cause the coagulation and flocculation of the suspended solids is proposed, which leads to higher COD and TS reduction than the reductions possible with the existing process. An extra step is taken for the treatment of the waste with the implementation of membrane technology. Ultrafiltration did not alter significantly the waste but removed all the larger suspended solids, preparing it for the step of reverse osmosis.

With the use of a reverse osmosis membrane, the organic content of the waste is dramatically reduced to a value of around 30 mg/L, and the final effluent is suitable for recycling, irrigation, or disposal to water banks. Fouling phenomena are apparent, but further experiments must take place in order to find the experimental conditions that minimize such problems.

PART B: Carbon nanotubes and polymeric membranes

3. Theoretical background

Since thirty years of research, carbon nanotubes abbreviated by CNTs acronym are dominating in the new materials world and they are revealing an enormous potential of hundred different possibilities and applications. Andre Geim and Konstantin Novoselov were awarded 2010 Nobel Prize for their work on carbon sheet of graphene and this is not a matter of chance but fact of a real new age beginning for material engineering. Membranes of different polymers embedded with clouds of single or multi walled carbon nanotubes raise new efficiency standards and expectations. The innovative membranes can be considered as a good alternate solution for both tap water and wastewater treatment via already applied processes as ultrafiltration, nanofiltration and reverse osmosis.

3.1 Carbon nanotubes

Carbon nanotubes (CNTs) are hollow and more than 50.000 times thinner than a human hair (15). CNT is simply a nanometer-sized rolled-up atomically smooth graphene sheet that forms a perfect seamless cylinder capped at the ends by fullerene caps (8).

A single-walled carbon nanotube (SWCNT) is a single graphene sheet rolled into a seamless cylinder with either open or closed ends. Multi-walled carbon nanotubes (MWCNTs) are two or more concentric cylinders of graphene sheets of successively larger diameter, forming a layered composite tube bonded together by van der Waals forces, with a distance of approximately 0.34 nm between layers. In the market, average diameter of a single-wall carbon nanotube typically ranges of 0.6 nm to 100 nm. The aspect ratio, i.e., length to diameter, typically ranges from 100 to 1000. A nanotube of 2 nm diameter has a length of 100 to about 1000 nm. In preferred embodiments, the average length is from about 200 nm to about 1000 nm.

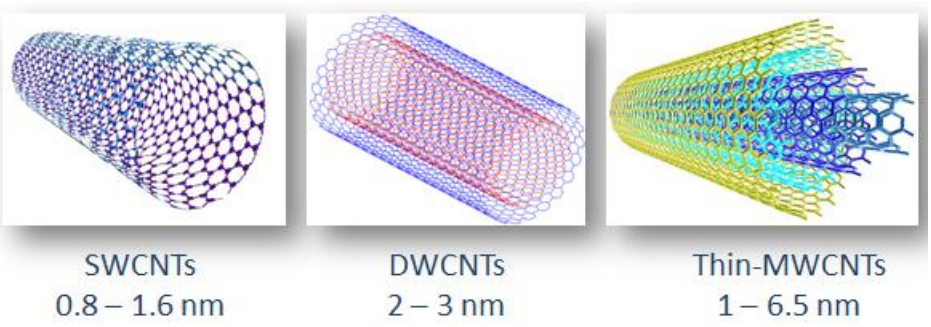

Figure 12 Different types of pristine carbon nanotubes and inner diameter (9)

For reverse osmosis, and notably for water desalination, a preferred inner diameter range is about 0.4 nm to about 5 nm (Figure 12), and a most preferred range is from about 0.4 nm to about 1.2 nm. For nanofiltration membranes, a preferred size range is from about 1 nm to about 10 nm. For ultrafiltration membranes, a preferred size ranges from approximately 5 nm to about 200 nm (8).

3.2 Modification

Carbon nanotubes are modified by alcoholic group –COOH in their external part leading to hydrophilicity nature and improving water contact on the surface of the membrane. Therefore modified CNTs offer improved electrostatic effect with metal ions containing in water and wastewater and more chirality effect with functionalized groups are appeared (11). Certain improvements are observed as a function of CNT functionalization and most importantly CNT volume fraction. It is proved in the literature that CNTs with larger diameter are more effective to remove organic molecules (11), (18). For water the pore diameter is related to the higher flow through the pores. Deprotonation reaction modifies COOH to COO^- with negative charge. CNTs with COO^- functional group causes charge effects, improves stabilization of solution, has better water dispersion and probably rejection factor for some sorts of foulants and pollutants.

3.3 The four mechanisms model

Mixed matrix membranes are created on the cross point of different physical phenomena enable to provide them with great separation properties. The inner cavity of CNTs forms a natural pore with very small diameter that can in some instances be smaller than 2 nm. This pore works as a both side passage for fluids and retain greater molecules by size exclusion mechanism and diffusion solution model explains water movement inside the pores.

Moreover, smooth hydrophobic surfaces of the nanotubes lead to nearly frictionless flow of water through them, enabling transport rates orders of magnitude higher than transport in conventional pores (11), (15). The structure of CNTs permits targeted specific modifications of the pore entrance without destroying the unique properties of the inner nanotube surface. Charge effects occur between functional groups attached carbon nanotubes edges contributing increasing molecules interactions (12). The combination of these three factors: size exclusion, hydrophobic environment and charge effects make mixed matrix membranes or membranes embedded with CNTs enable membranes efficiency in numerous applications improving rejection factor, extending lifetime and improving flux permeability (13). Another mechanism which appears quite often is sorption of molecules inside CNTs empty sites depending on the nature of molecules of pollutants.

In details, the four mechanisms which act simultaneously are described below:

- **Size exclusion: Ultrafiltration applications**

The membrane is in this case a filter plate with holes (pores) that are too small for the particles to pass but big enough for the fluid to permeate easily. Permeation of a molecule through an ideally permeable membrane occurs without energy dissipation. In ultrafiltration, the carbon nanotube wall acts as a filter for all particles larger than 0.01 micron: pollen, algae, parasites, bacteria, viruses, germ and large organic molecules (15). In literature, CNTs membranes prove selectivity close to 100% for different molecules (15).

- **Surface interactions: Adsorption effects**

Filtration by CNTs pores occurs for the larger sized macromolecules, but sorption dominating for the medium molecular weight organics. On the surface of CNTs, free spaces provide adsorption sites for small molecules in solution (13). The data for the hydrocarbons show some evidence for sorption effects occurring inside the pores. In wastewater of paint industry metallic ions can be adsorbed or retained in these pores (12).

- **Ion exclusion: Charge effect**

Polar groups (eg –COOH) are attached on the surface of membrane or in the end of carbon nanotubes by chemical modification (see modification part) in order to improve charge interactions in case of charged molecules (metal ions). Polar groups enhances adsorption desorption and ion exchange in high pH solution (17) and increase the flux. Mesoporous membranes that have a charged pore surface in salt solutions may exhibit significant ion

retention by a space charge effect if pore size is smaller than the Debye length of the solution.

- **Water transition: Hydrophilicity-Hydrophobicity effects**

In case of mixed matrix membranes or membranes embedded with CNTs the water molecules just fit inside the pore and apparently have significant mobility with respect to the pore wall (18). By simulation models, water appears to move like a solid (19) inside the tube making a hydrogen bond wire wherein the hydrogen bonds literally move between the hydrophobic walls and they try desperately to escape. Water molecules inside and outside the nanotubes are in thermodynamic equilibrium (15).

3.4 Computer simulations

The flux of charged and neutral molecules is studied thoroughly using modelling tools by Luca and Voyiatzis group in Institute of Chemical Engineering Sciences in Patras (19). The first question one may ask is why does water wet CNTs. The study showed that water flow is limited mainly by particle entry and exit events, and that tube length had hardly any effect. For far small SWNT studied by Hummer et al., carbon nanotubes of very small diameter (0.8nm) have so narrow passage that only a single water molecule could be inserted, forming a single file water chain (19). Hummer et al. further noted that this wall friction appears to be exceedingly small, as in the gas-diffusion case. Indeed, graphite is an industrial-grade solid lubricant. Monte Carlo simulations show that a defining feature of the water structure in CNTs is the formation of the hydrogen-bonded “water wires” oriented along the nanotube axis (12).

3.5 Sonication

Sonication is the process of converting an electrical signal into a physical vibration that can be directed toward a substance and it is the act of applying sound (usually ultrasound) energy to agitate particles in a sample (21). Sonication effect enhances formation, growth, and implosive collapse of bubbles in a liquid. In the laboratory, it is usually applied using an ultrasonic bath or an ultrasonic probe, colloquially known as a sonicator. The primary part of a sonication device is the ultrasonic electric generator. This device creates a signal (usually around 20 KHz) that powers a transducer. This transducer converts the electric signal by using piezoelectric crystals, or crystals that respond directly to the electricity by

creating a mechanical vibration. This vibration, molecular in origin, is carefully preserved and amplified by the sonicator, until it is passed through to the probe. The sonication probe transmits the vibration to the solution being sonicated. Probe is a carefully constructed tip that moves in time with the vibration, transmitting it into the solution. The probe moves up and down at a very high rate of speed, although the amplitude can be controlled by the operator and is chosen based on the qualities of the solution being sonicated. The rapid movement of the probe creates an effect called cavitation. Cavitation occurs when the vibrations create a series of microscopic bubbles in the solution, pockets of space wedged between the molecules that form and then collapse again under the weight of the solution, sending out tiny shockwaves into the surrounding substance. Thousands of these bubbles forming and collapsing constantly create powerful waves of vibration that cycle into the solution and break apart i.e. cells or in case of carbon nanotubes, long chain of carbon nanotubes are separated (21).

At the beginning of sonication, MWCNTs exist as big aggregates and bundles in solution that are strongly entangled, and no absorption is evident in the UV–vis spectrum (24). During sonication, the provided mechanical energy can indeed overcome the van der Waals interactions in the MWCNTs bundles and lead to their disentanglement and dispersion.

3.6 Carbon nanotubes dispersion

The sonication-driven dispersion of carbon nanotubes in deionized water and aqueous surfactant solution has been monitored by UV–vis spectroscopy in water and surfactant solutions of CNTs after 5 months maturing. Time dependent sonication experiments reveal that the maximum achievable dispersion of CNTs corresponds to the maximum UV–vis absorbance of the solution (24). With higher surfactant concentration the dispersion rate of CNTs increases and less total sonication energy is required to achieve maximum dispersion. Dispersion of higher CNT concentrations requires higher total sonication energy. The surfactant molecules are adsorbed on the surface of the CNTs and prevent re-aggregation of CNTs so that a colloidal stability of CNT dispersions could be maintained for several months.

4. Experimental Procedure

4.1 Carbon nanotubes

In this project, carbon nanotubes are made by catalytic chemical vapour deposition using quartz probe CVD (13). Single carbon nanotubes (SWCNTs) have 1-2nm external diameter and 0.8-1.2 internal diameter. Thin multi walled carbon nanotubes (Thin-MWCNTs) have 1.0-6.5nm and 6-15nm inner and outer diameter respectively. SWCNTS and Thin-MWCNTs with different functional groups (COOH and COO^-) were provided from Nanothinx Inc when only SWCNTs are made by Cheaptubes company.

Table 8 Carbon nanotube types, physical and cost parameters used in the project

	SWCNT *Cheaptubes	SW-COOH	SW-COO^-	Thin – MWCNT *Nanothinx	T– MWCNT-COOH	T– MWCNT-COO^-
Carbon Purity (%)	>90	>90	>90	94	94	94
External Diameter (nm)	1-2	1-2	1-2	6 – 15	6 – 15	6 – 15
Internal Diameter (nm)	0.8 – 1.6	0.8 – 1.6	0.8 – 1.6	1.0 – 6.5	1.0 – 6.5	1.0 – 6.5
Length	5-30μm	≤ 1μm	≤ 1μm	≥ 10μm	≤ 1μm	≤ 1μm
Price (1 gram)	84 €	93 €	117 €	16 €	31 €	40 €

4.2 Dispersion of carbon nanotubes solutions

The surfactant used for the dispersion of the CNTs was pluronic F-127 (SDS; 90%) provided by Sigma Aldrich. All dispersion experiments were carried out with distilled water. All solutions were prepared by mixing a certain amount of CNTs with aqueous PF 127 solution in a flask, after which the resulting mixture was sonicated for different times under mild conditions. It is also notice that either via chemical or mechanical functionalization final length of carbon nanotubes reach 320nm and 550nm respectively and thus they can easily tuned in embeddement procedures (28).

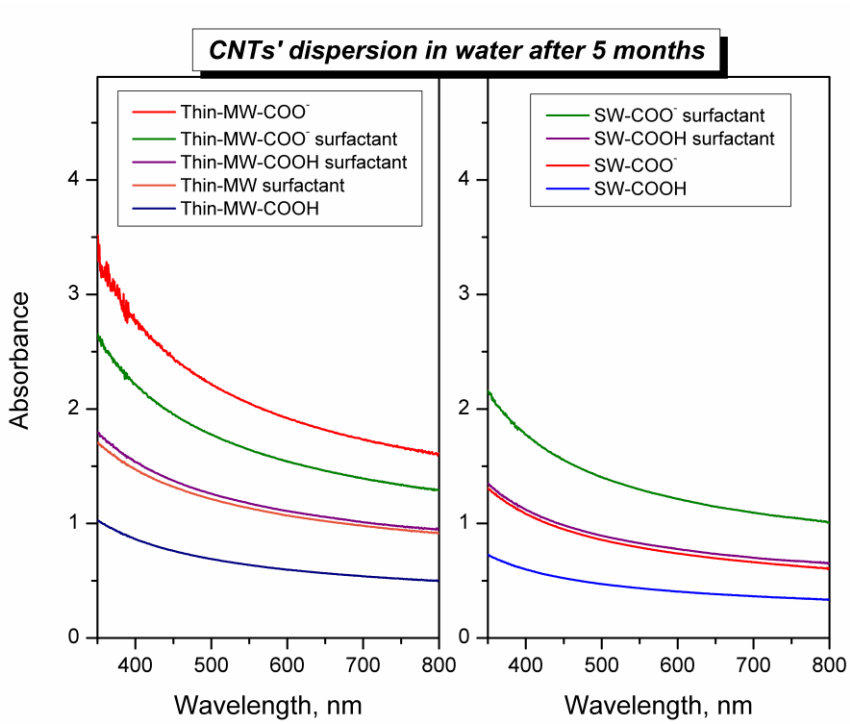

Figure 13 Evolution of UV–vis spectra of an aqueous 0.1 wt.% MWCNT–0.15 wt.% SDS solution as a function of sonication time at continuous power of 20 W (solutions are diluted by a factor of 150)

In spectrum made by UV spectrometer, bundled CNTs, however, are hardly active in the wavelength region between 200 and 1200 nm – their photoluminescence is quenched – most probably because of carrier are tunnelling between the nanotubes. Therefore, it is possible to establish a relationship between the amount of CNTs individually dispersed in solution and the intensity of the corresponding absorption spectrum. Moreover, UV-vis spectroscopy can be used to monitor the dynamics of this dispersion process of CNTs, allowing the determination of the optimal sonicating time. UV–vis absorption spectra were recorded with a Hitachi U-3000 spectrometer operating between 200 and 1100 nm. The blank used was deionized water.

Figure 14 illustrates UV–vis spectra of CNTS – water and PF 127 solutions. After sonication the absorbance of MWCNT solutions shows a maximum between 200 and 300 nm and gradually decreases from UV to near-IR, which is partly due to scattering, especially in the lower wavelength range. Similar results are reported for UV–vis absorption spectra of SWCNTs by Jiang et al. (24). The increasing amount of dispersed MWCNTs results in an increasing area below the spectrum lines representing the absorbance. Thin MW-COOH and SW-COOH CNTs in water exhibit lower absorbance – or either higher light transmission and

COO^- both SW and Thin MW in surfactant and water permit higher absorbance and lower UV transparency. Consequently, Thin MW-COO^- in water and SW-COO^- in surfactant can be considered as best dispersed and stable mixtures of CNTs after 5 months.

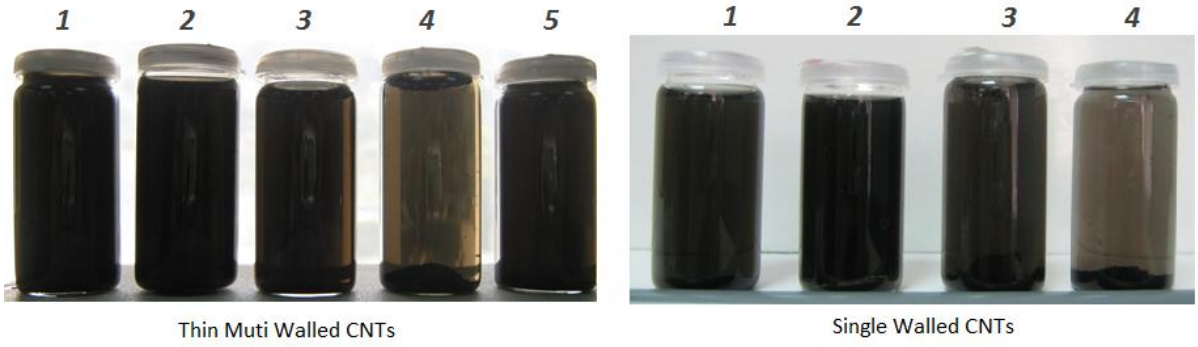

Figure 14 CNTs dispersion in water solutions after 5months (Thin Multi Walled CNTs where 1) Thin-MW-COO- 2)Thin-MW-COOH 3) Thin-MW-COOH and surfactant 4) Thin-MW-COOH 5) Thin-MW and surfactant & Singe Walled CNTs 1) SW-COOH and surfactant 2) SW-COO0 and surfactant 3) SW-COO- 4) SW-COOH

4.3 Deprotonation

MWCNTs and SWCNTs are functionalized in a mixture of NaOH to increase their dispersion in organic solvents (11). The typical approach is as follows; 500mg Thin-MW-COOH are washed in 400mL 3times deionised water before and left to dry at room temperature in ultrafiltration unit using polycarbonate filter. Washing is repeating for three times.

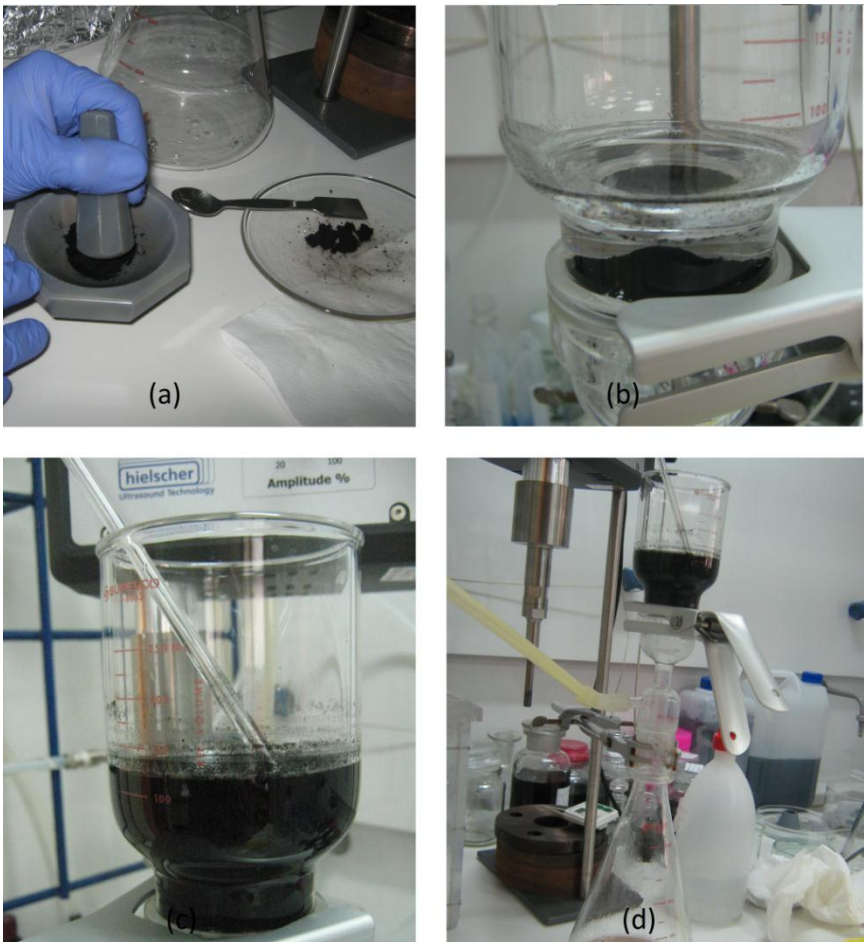

Figure 15 Deprotonation method by (a) smashing dried CNTs -COOH (b) washing CNTs with water (d) rinsing with NaOH solution (d) filtrated CNTs in ultrafiltration unit with polycarbonate filter

The dried MWCNTs are then refluxing in 50mL NaOH (10%wt NaOH in water) and mixture is then ultrasonicated for 10min. Step is repeating three ties. Finally, the Thin-MW-COO^- CNTs are washed and filtered until the pH value of the solution reached 7.0 and again dried in oven at 60^oC overnight.

4.4 Ultra sonication

All sonication processes in this project carried out with a horn sonicator (Sonic Vibracell VC750) with a cylindrical tip (10 mm end cap diameter). The output power was fixed at 20 W, thus delivering energy of 1100–1200 J/min.

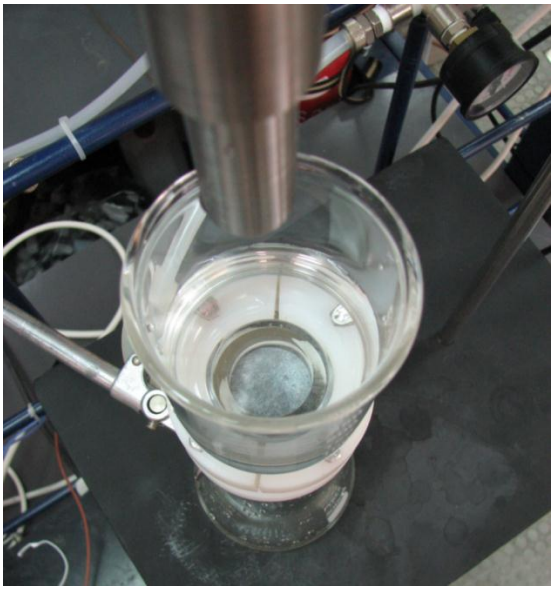

Figure 16 Sonication pin over ultrafiltration unit in laboratory

5. Membranes embedded with carbon nanotubes

5.1 Polyvinylidene Fluoride (PVDF) membranes

Commercial Polyvinylidene Fluoride (PVDF) membranes are used in ultrafiltration configuration varying carbon nanotubes concentration in tip sonication solution. Durapore® membranes are provided by Sigma Aldrich and product specifications are given as following: PVDF membranes, pore size 0.1µm and 47mm diameter, white colour and plain surface, thickness 125µm, sterilization by autoclave at 121^{o}C, operating temperature 85^{o}C, bacterial endotoxins 0.5EU/mL (22). Durapore give low extractability and broad chemical compatibility. Hydrophilicity of PVDF membranes in water solution is hydrophilic binding less than nylon, nitrocellulose or PTFE membranes.

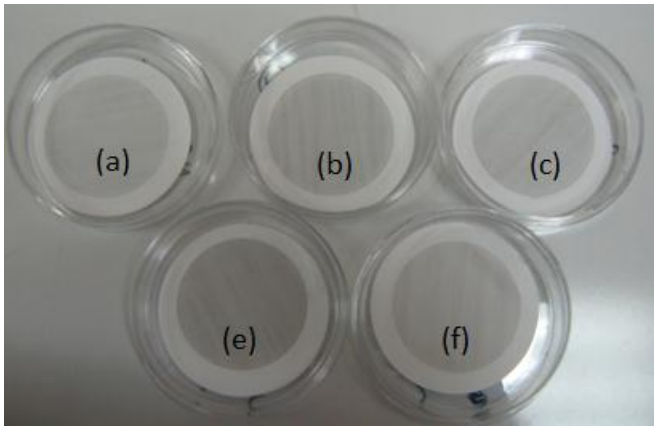

Figure 17 PVDF membranes embedded with carbon nanotubes solution of concentration: 0.1µg/L (b) 0.3 µg/L (c) 0.5 µg/L (d) 0.7 µg/L (f) 0.9 µg/L (e) 1.1 µg/L (f) 1.3 µg/L

Figure 18 Ultrafiltration unit in laboratory (pressure supply, vessel, and membrane)

The membranes have been embedded with CNTs solution of different concentrations from 0.1µg/l to 1.3µg/l. Embeddement with several concentrations of thin MW-COOH carbon nanotubes has been made at 0.2bar. The results are grouped in next figure.

Table 9 Measured permeability for distilled water through bare PVDF membranes and PVDF membranes embedded with different concentration of Thin MW-COOH CNTs

Concentration (µg/mL)	Permeability before CNTs [L/m^2·h·bar]	Permeability after CNTs [L/m^2·h·bar]
0.1	5141	5126
0.3	5340	5340
0.5	5423	5066
0.7	4957	4773
0.9	5149	5103
1.1	5149	5315
1.3	5141	4901

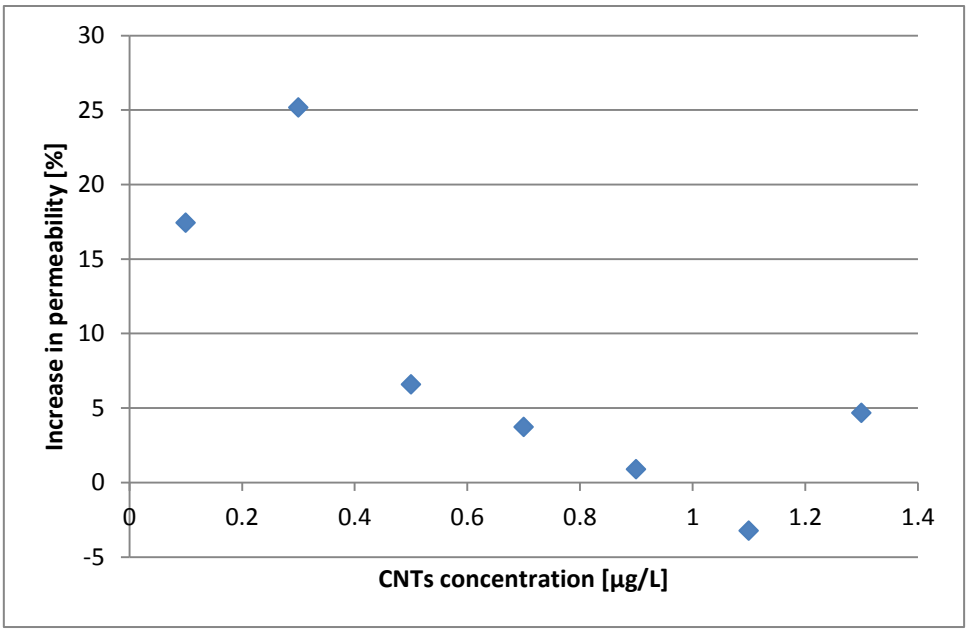

Figure 19 Flux increase (%) in function of CNTs concentration in solution of embeddement

By Figure 19, highest flux is observed at 0.5µg/L carbon nanotubes. The flux increases 27% using carbon nanotubes in PVDF pores by tip sonication embeddement and water permeability increases 6.5%. By literature (23), low or super low concentration proves better result and main cause can be fouling effects inside the pores of polymeric membranes. Although 27% higher flux of PVDF membrane, the result cannot get beyond normal polymeric membranes efficiency or either in terms of cost and environmental risks.

Repetition of experiment for 0.3µg/L tried to optimize the process and verify CNTs contribution. Under same experimental conditions, 0.2bar and thin MW-COOH CNTs three more PVDF membranes have been tested for 0.3µg/L CNTs concentration. The flux reduction is measured in ultrafiltration configuration and new results show no increase of

flux in any case and either decrease of flow, approximately 4%. Fouling effects and typical measurement errors might be the source of insufficient results.

5.2 Sonication effect

In order to evaluate tip sonication impact in pores geometry, a series of experiment with two different duration of sonication has been carried out. PVDF membranes have been sonicated for 2min and 7min. Flux has been measured in both cases and in both cases flux after sonication is lower. Consequently, there is not positive impact in flux increase by the tip probably because of spreading effect of sonication in membranes pores or crack effects.

Table 10 Results of permeability change for distilled water in ultrafiltration unit before and after tip sonication

	Permeability before tip sonication [L/m^2·h·bar]	Permeability after tip sonication [L/m^2·h·bar]
2min of sonication	4245	3995
7min of sonication	4233	4150

PVDF membranes shown poor results and further study on PVDF membranes embeddement is not imposed at this point. However other type of polymers need be tested in terms of CNTs fouling effect, permeability and pollutants exclusion.

5.3 PES/PET membranes

Commercial PES/PET membranes are used for embeddement with CNTs. Microdyn Nadir Membranes UP150 purchased by Microdyn Nadir company have nominal properties as following: Ultrafiltration, PES side, 150kDa molecular weight cut off (MWCO), 40nm pore size, 200μm thickness and they combine PES and PET layers. PES side works like filter and PET is the support layer. Nominal water flux of UP150 is 200L/(m^{2}h).Geometry of PES/PET in terms of pores is conical where PET has large diameter pores and PES smaller one.

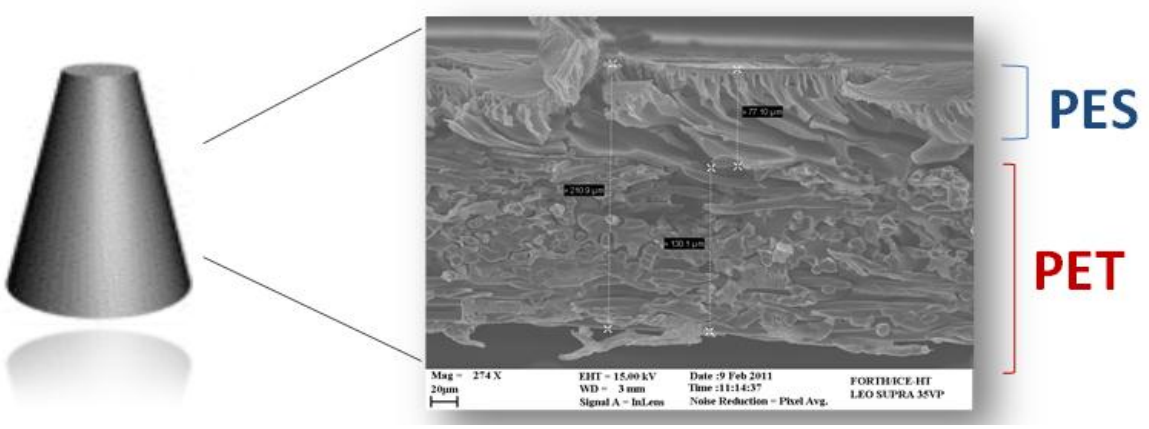

Figure 20 UP150 PES/PET membrane geometry of pores and PES/PET layers in SEM image

Target pore size is defined to 1.5-2nm and 0.1-3kDa MWCO. Appropriate carbon nanotubes need to have diameter in scale of target pore size as Thin MWCNTs functionalized with OH, COOH 1.0-6.5nm of internal diameter, DWCNTs 1-2nm of internal diameter and SWCNTs of 0.8-1.6nm internal diameter. Target pore size need to be in same size with internal diameter of carbon nanotubes. Due to UP150 conical structure, CNTs attached at PES are able to stay on PES side or might stack there. Otherwise, if CNTs move on PET side and PET side embeddement take place, CNTs cross the path inside PET-PES pore and appear on the PES side of the membrane. In the laboratory, experiments have already proved last argument.

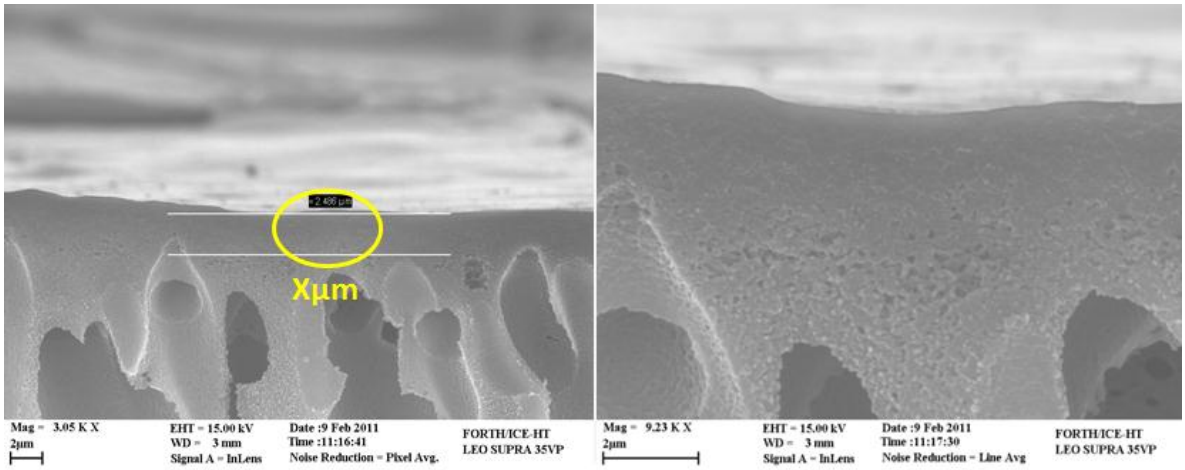

Figure 21 UP150 Active layer PES side cross section image by SEM. Thickness of active layer measured to 2.488µm

The optimal case is to infiltrate CNTs across PES selective thin layer. However, due to anisotropic, sponge like character of the porosity of this thin layer, infiltration is quite demanding and thus optimization of the method is required.

The configuration of rectangular membranes embeddement consists of lab made vessel in scale of UP150 membranes 1600mL, pressure supply, ultrafiltration configuration, membrane, metallic sieve, sealer made by silicone.

Figure 22 Tip sonication and ultrafiltration configuration. Rectangular vessel contains CNTs solution which by pressure difference is driven through membrane pores

5.4 Optimization of PES/PET embeddement

Experiments have been carried out in the past also by PET side. In that case carbon nanotubes have emerged in PES side with 2μm distance and this is what called the active side of the membrane. In older experiments of the group, PES side and SWCNTs 2.5 μg/ml gave 14.6% increase in water flux permeance when for PET side and SWCNT's 2.5 μg/ml percentage raised to 32.40%.

In this project, different concentrations of CNTs are applied aim to optimize water flux and rejection properties of UP150 membranes. Thin MW COO^- CNTs and SW have shown fine dispersion behaviour, suspension concentration is 100μg/mL and CNT density is 384μg/cm^2. Isopropanol water solution (1:4) is prepared to enhance opening pore of membranes.

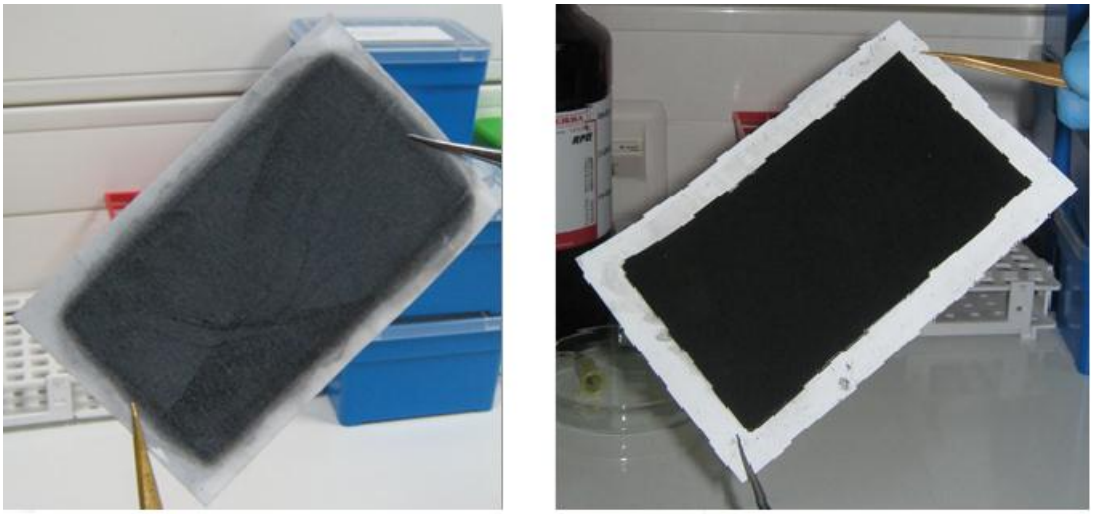

Figure 23 UP150 PES/PET membranes infiltrated with (a) SWCNTs and (b) Thin MW-COO- by PES side

Before tip sonication of CNTs solution, SWCNTs are mixed with Sodium Dodecyl Sulphate (SDS) surfactant 1:1.5 and for Thin MW-COO^- dispersion experiments have proved no surfactant is needed. For SWCNTs tip sonication took 5 min in order to open CNTs paths and for Thin MW-COO^- tip sonication took 7 min. Pressure supply for embeddement is 0.5bar. Tip sonicator stand slightly high and CNTs solution is adding drop by drop in order to achieve better dispersion, opening and homogeneity of solution. Tap water is used (10mL containing 667μg CNTs, hence final solution is 0.312 μg/mL at 1600mL). Ultrafiltrating membrane with 300mL dispersion is embedded, thus final density on membrane surface is 1.6μg/cm^2. Ultrafiltration of 300mL takes 2.5min and PES side starts change to grey because of CNTs.

Table 11 Suspension concentration and composition for PES/PET membranes embeddement

	CNT type	Surfactant	Suspension concentration [μg/mL]	CNT [μg/cm^2]	REMARKS
Infiltration parameter from PES side Rectangular UP150 membrane 6.5x12cm	Thin MW-COO^-	SDS	0.312	1.6	5 items
	SWCNTS		0.312	1.6	5 items

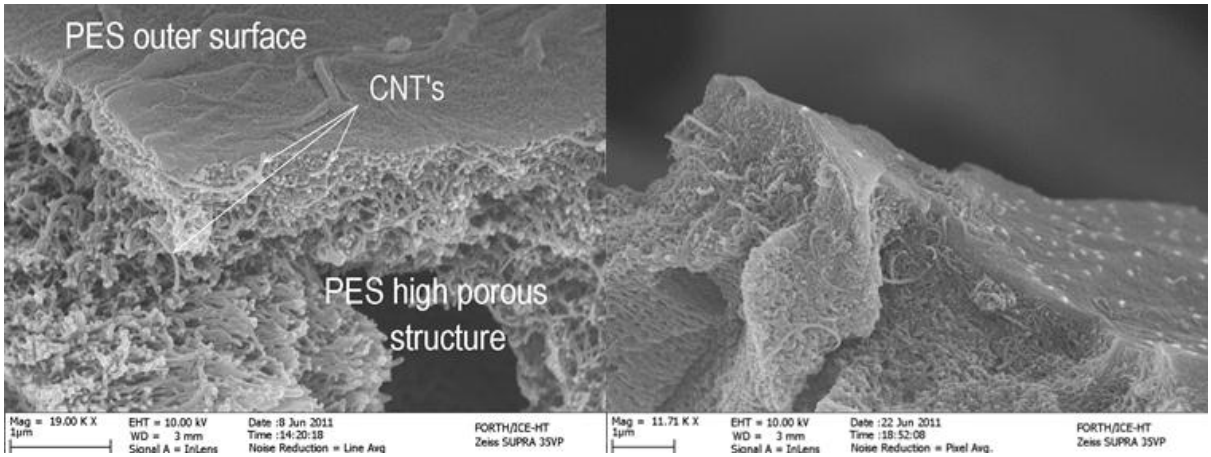

Figure 24 Images of cross sections of PET side of membranes infiltrated through the support, with Thin-MW-COOH or SW CNTs (10)

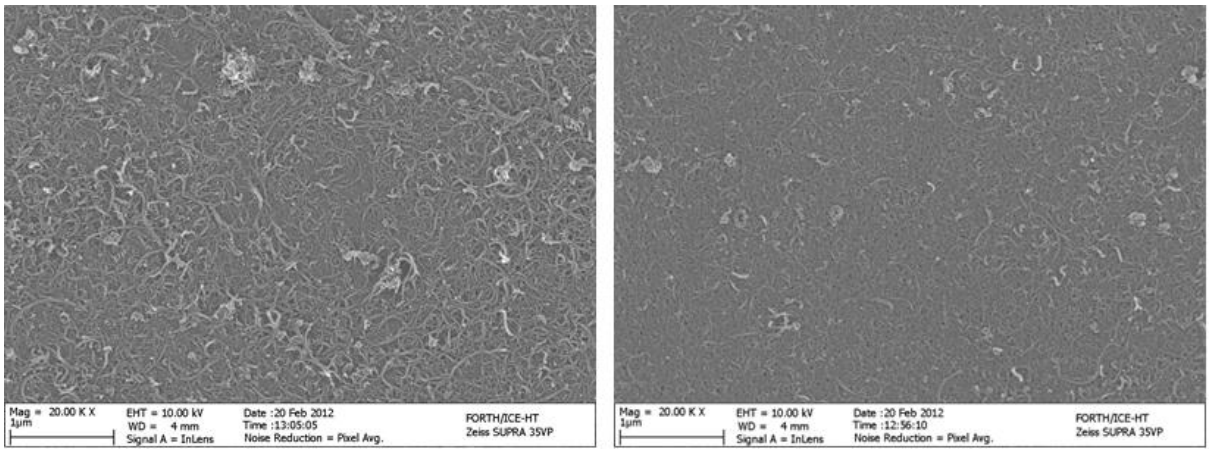

Figure 25 Images of the surface exposed to the feed from membranes infiltrated through the thin selective layer side, with Thin-MW-COOH or Thin-MW-COO-

In Figure 25 the embeddement of carbon nanotubes inside the pores and over the PES area is well illustrated. A homogenous distribution of carbon nanotubes is also achieved.

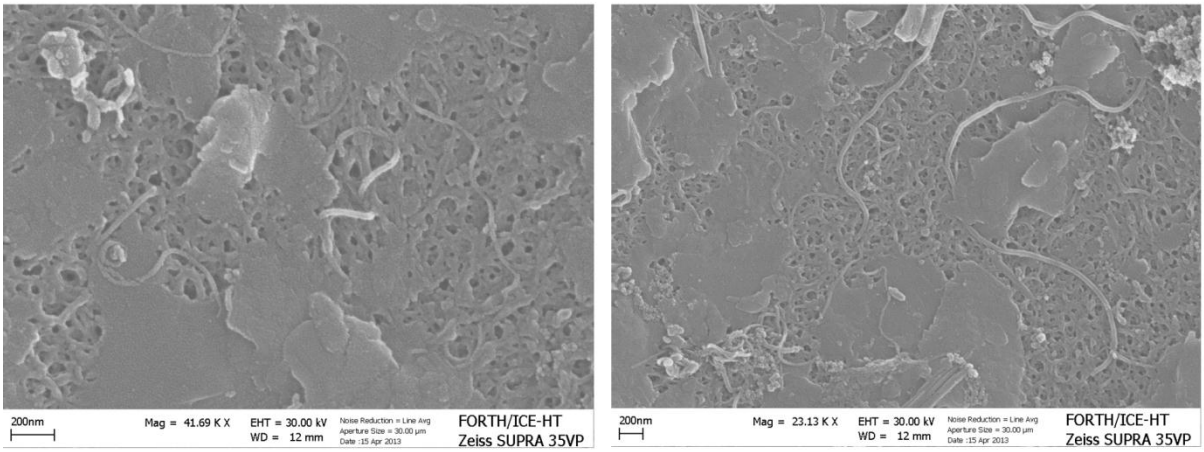

Figure 26 UP150 membrane infiltrated with Thin-MW-COO- CNTs 0.312 μg/mL (1.6 μg/cm^2) from PES side

Membranes incorporated with Thin MW-COO$^-$ CNTs 50μg/mL can be covered with PVDF layer 0.1% w/v in MeOH have shown tendency to increase pure water permeability in comparison with commercial UP150 PES/PET membrane. Experiments are repeated in order to evaluate Thin MW-COOH CNTs geometry over PES layer. Tip sonication to the mixture took 25min in order to separate sufficiently carbon nanotubes. Surfactant used was PF127 1:1. Isopropanol solution (1:4 in water) removed glycerine layer over PES/PET membranes before ultrafiltration. PVDF coating tried to apply over PES/PET embedded membranes with spin coating – phase inversion method (see below). However process is simple and promising, PVDF does not show enough adhesion over PES and other methods might need to be studied.

5.5 Permeability of deprotonated CNTs incorporated from PES and PET sides of UP150 membranes

The UP150 membranes with PES on the surface and PET as support layer were infiltrated with deprotonated thin walled CNTs (Thin MW-COO$^-$) and were tested on laboratory OSMOTA test unit at HSKA, Karlsruhe, Germany for the pure water flux as well as for the flux with model textile wastewater (MTWW). The flux from the deprotonated CNTs incorporated inside PES and PET surface were compared to the commercial membranes under similar operating conditions of 1.5-2 bar pressure and 0.4 L/min of cross-flow velocity. For functionalized CNTs incorporated from PES side of UP150 results verified an increase of permeability in pure water relatively high (above 1400 L/m$^{2\cdot}$h·bar) initially. Need to point

out that a great loss of deprotonated CNTs was noticed while treating with glycerol as well in the solution from these set of CNTs embedded membranes. The pure water flux as well as the flux from the MTWW, tested on our laboratory unit was compared to the pure water flux from commercial membranes as shown in Figure 27.

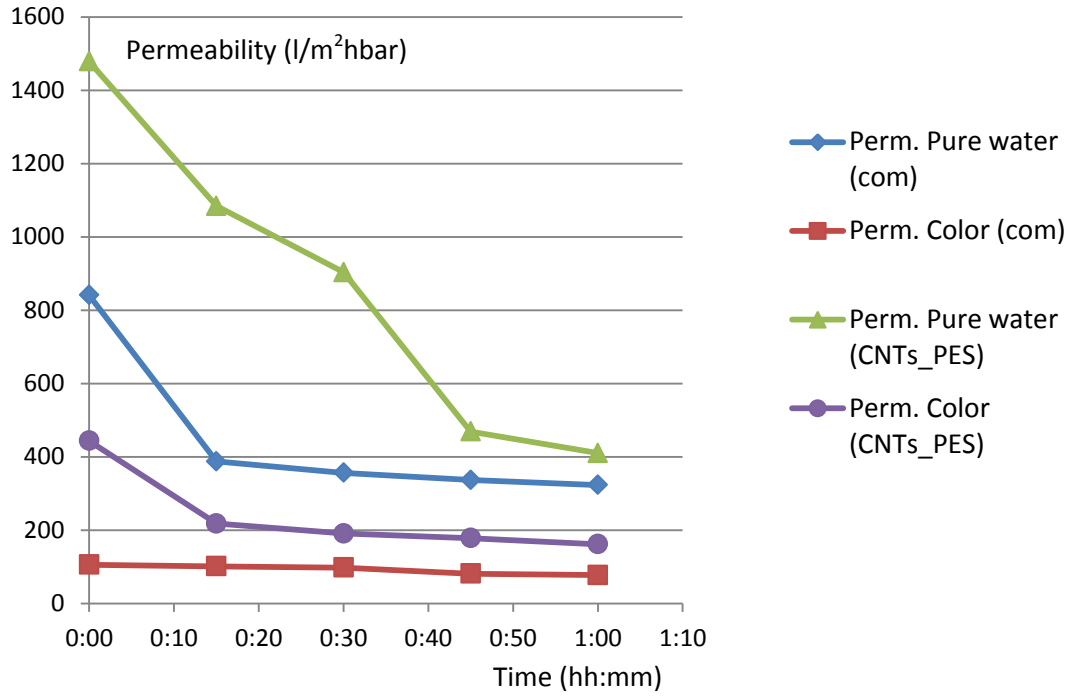

Figure 27 Permeability vs time plot of commercial and CNTs embedded MN membranes (com:commercial UP150, CNTs_PES:UP150 with CNTs incorporated from PES side)

The permeability of deprotonated CNTs incorporated through PES side was around 409 $L/m^{2}{\cdot}h{\cdot}bar$ while that of commercial membranes is 323 $L/m^{2}{\cdot}h{\cdot}bar$ when treated and operated under similar conditions. The permeability with MTWW was around 160 $L/m^{2}{\cdot}h{\cdot}bar$ while that for commercial membrane was 80 $L/m^{2}{\cdot}h{\cdot}bar$. Infiltration of functionalized CNTs from PES side showed significantly higher permeability when compared to the commercial membranes. However, the rejections of red and blue colour from UV-vis spectrometer measurements display 0.8 and 1.65 % respectively while that of commercial membranes was noticed to be 17.55 % for red while 22.35 % for blue respectively.

Carbon nanotubes incorporated from PES side (small pore hydrophilic surface) give promising results in permeability. Losses of CNTs during permeability experiments need high concern in case of membrane use in potable water purification applications. SEM images

pose important questions on CNTs penetration inside PES pores and thus further optimization is needed. Thin MW COO^- CNTs have slightly better consistency than SWCNTs given imaging characterization. Low concentration of embeddement solution is indeed an optimal choice at this point of study in terms also of cost saving in raw materials.

5.6 PES membranes with CNTs with Spin coating method

Single walled and thin multi-walled COO^- carbon nanotube and polyethersulfone blend membranes (also called as mixed matrix membranes) are synthesized via the phase inversion method (25). The resultant membranes are then characterized by scanning electron microscopy (SEM), gel permeation chromatography (GPC), ultrafiltration flux and water vapour permeability method. The mixed matrix membranes appeared to be more hydrophilic, with a higher pure water flux than the polyethersulfone (PES) membranes and give better size exclusion results for model foulants of PEGs. Therefore, it was noticed that the amount of CNTs in the blend membranes was an important factor affecting the morphology and their permeation properties.

Polyethersulfone (PES) membranes are synthesized via the phase inversion method using spin coater to create PES thin layer. A PES solution is prepared with 7%w/v polyethersulfone in dimethylformamide (DMF) solvent. The mixture was well stirring for 2h at room temperature. Two different solutions of SWCNTs and Thin MW-COO^- are prepared with N-Methyl-2-pyrrolidone (NMP) solvent to obtain 0.5% wt. CNTs respect to PES (0.035gr of CNTs for 7gr of PES in 100mL of solution). CNTs solution are mixed on stirring apparatus at room temperature and mixed are sonicated for good dispersion of CNTs. After dispersing CNTs in solvent, PES (20 wt. %) was dissolved in the dope solution by continuous stirring and heating at 60^oC until the solution became completely dissolved and homogenous. Mixtures are finally mixed and well stirring overnight.

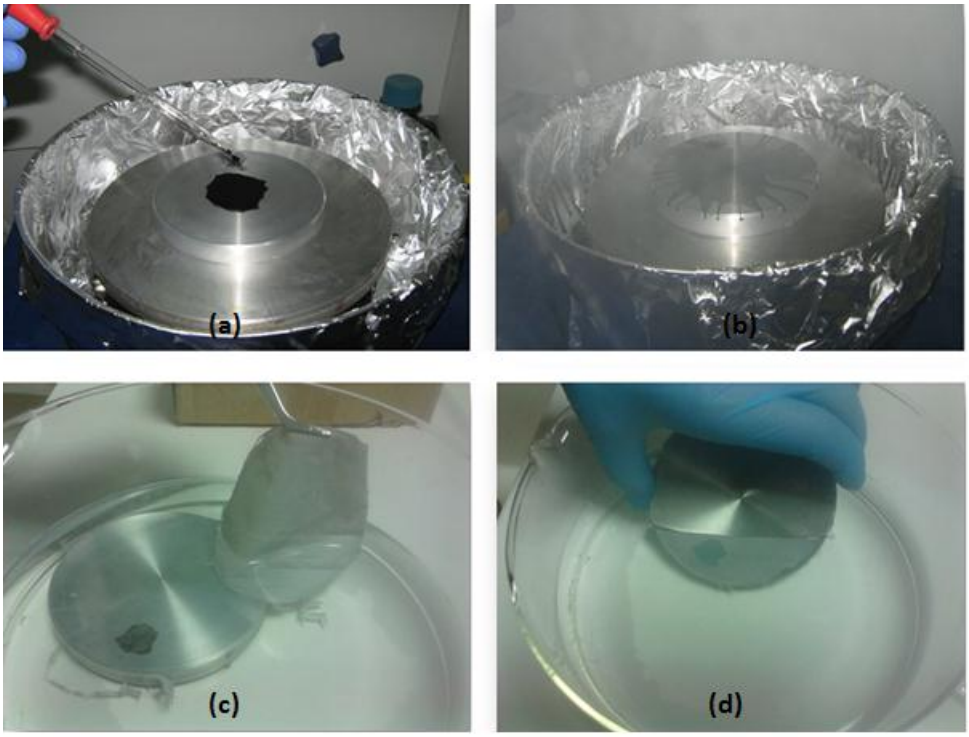

Figure 28 Spin coater and phase inversion in water for PES-CNTs membrane preparation (a) drop by drop PES-CNTs mixture over spin coater (b) fast round movement 300m/min for some seconds (d) & (c) phase inversion in water

Some attempts on spin coating shown that 7% solution of PES was quite thin and no dense layer could be created over spin coater because polymer was splitting around. Thus, increase of PES density is decided to 10% and new experiments show good adhesion of solution over metallic base of spin coater. Three different mixtures (PES% wt., PES with SWCNTs, PES with Thin MW-COO^-) are prepared. Over thin metallic layer, mixture is dropped in each case and spin coating run for approximately 20sec in 300m/min circular velocity. Metallic plates are directly immersed in tap water and phase inversion appeared after first seconds. The formed membranes were subsequently washed with deionised (DI) water and stored in DI water until use.

Figure 29 Lab made membrane with phase inversion and spin coating method with bare PES 10%w/v (left side) and SWCNTs 0.5%wt. (right side)

Results of carbon nanotube penetration via PES polymeric channels are tested via four different characterization methods: Water permeability in ultrafiltration unit, SEM images, water vapour permeability and gel permeation chromatography (GPC).

A. Water permeability

Water permeability is measured via lab ultrafiltration unit with 0.2bar pressure supply filling 1L water in vessel and measuring water reduction in 12min. Membrane area is considering 0.078m^2.

Table 12 Water permeability results for PES-CNTs membranes made by phase inversion method

Spin coating membranes	Thickness [µm]	Tap water permeability [$L/m^2 \cdot h \cdot bar$]
PES membrane	95	737
	95	1923
	35	1041
PES Thin $MWCOO^-$	70	2500
	70	1000
	40	3205
PES SW-COOH	130	4006

Spin coating membranes	Thickness [μm]	Tap water permeability [L/m^2·h·bar]
	27	2082

By Table 12, though tap water permeability does not follow a clear relation in function with thickness or membrane material, it is clearly assumed that mixed matrix membranes with carbon nanotubes give higher permeability. For PES Thin MWCOO$^-$ membrane, thinner membrane (40μm) show highest permeability (3205 L/m^2·h·bar) where for PES SW-COOH, thick membrane (130μm) achieve a quite high permeability (4006 L/m^2·h·bar). Hence, thickness cannot be considered as a crucial factor though it is quite important in terms of commercial use of layer. In case that PES Thin MWCOO$^-$ layer need to cover UP150 PES/PET membrane need to have less than half support layer thickness (200μm).

B. SEM images

In SEM images, carbon nanotubes appeared to be penetrated on polymer channels. However in cross section shots bulk material has no noticeable carbon nanotubes inside.

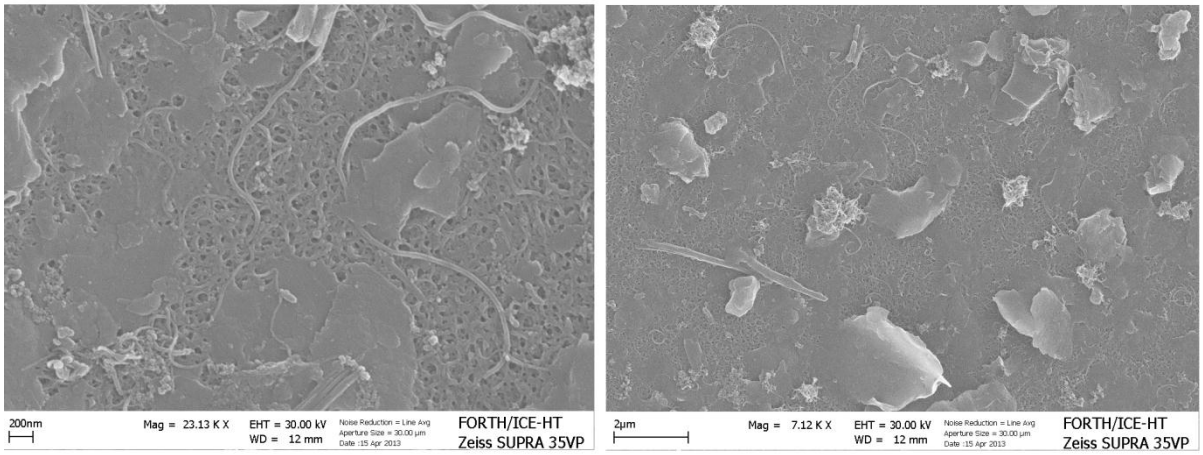

Figure 30 Mixed matrix membrane PES/Thin MW-COO- 0.312μg/mL

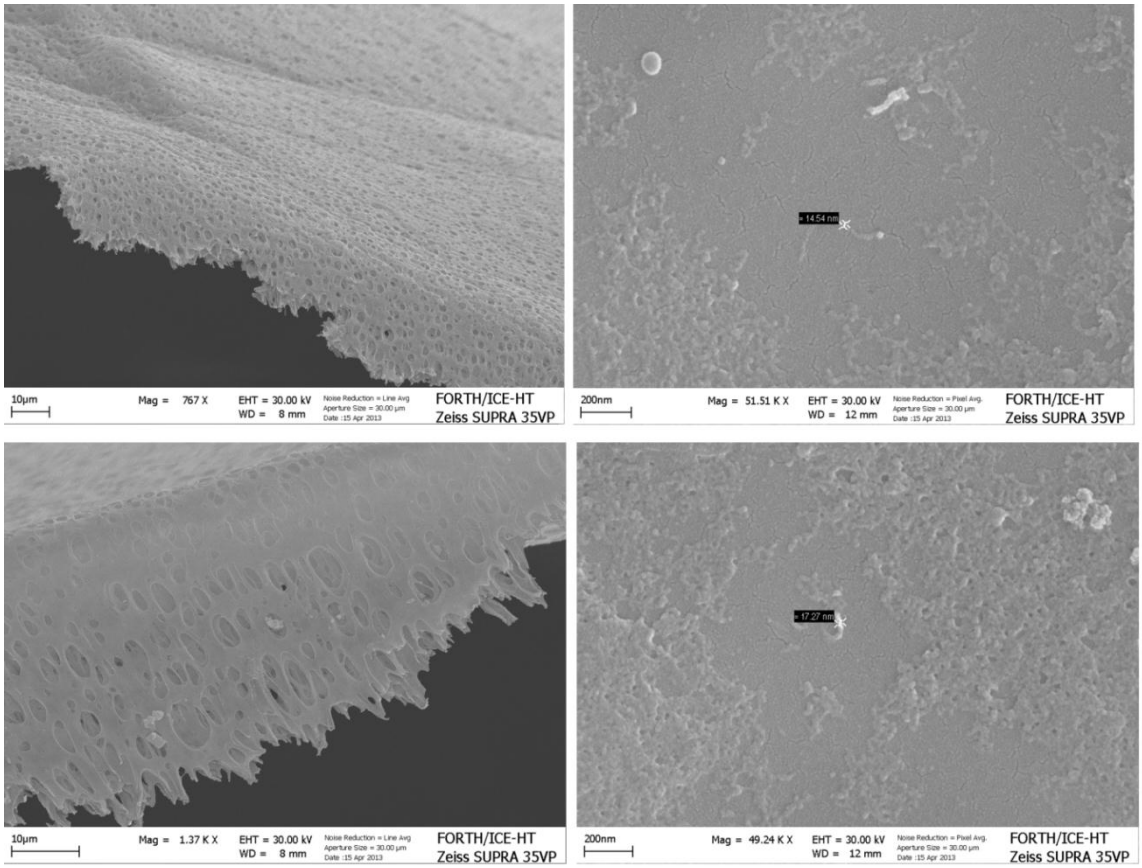

Figure 31 Mixed matrix membrane PES/SW-COOH 0.312µg/mL

Pore size of PES-SWCNTs has well defined with value of 10-15nm and clear pore channel of polymer. For PES-Thin MWCNTs COO^- pores are slightly larger, around 40nm when for pure PES membrane stable porosity can be concluded. Dye industry molecules and macromolecules vary in size but start above 60-80nm thus membranes blended with CNTs should be a physical barrier apart from sorption or chare phenomena.

C. Water vapour permeability

Pressure difference (ΔP) in stable temperature conditions in the two sides of the membrane comes from humidity difference and works like driving force for water vapour permeation through the membrane (26). The final result of the process is the weight losses of water existing in the container. Protocol of the method is described in ASTM E-96. Water Vapour Transmission Pressure (WVTR) is expressed via following equation (26):

$$\text{Specific WVTR} = \text{Thickness of film } (\mu\text{m}) \times \frac{\text{Water Weight Losses (gr)}}{\text{time (day)} \times \text{membrane area } (\text{m}^2)} \ [\text{gr} \times \mu\text{m} \times \text{day}^{-1} \times \text{m}^{-2}]$$

$$\text{Permeability} = \frac{\text{Specific WVTR}}{\Delta P}\ [\text{gr} \times \text{s}^{-1} \times \text{cm}^{-1} \times * (\text{cmHg})^{-1}]$$

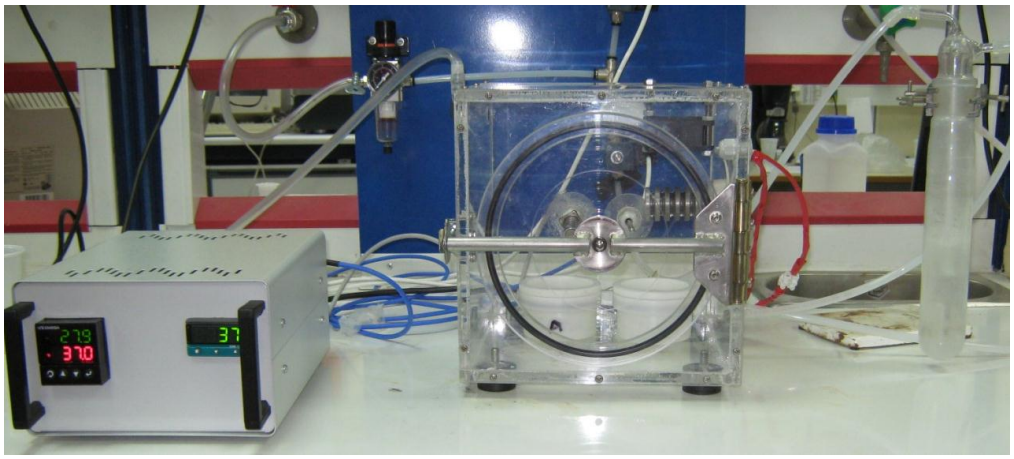

Figure 32 Water Vapour Transmission Permeability Apparatus in Laboratory

One PES membrane and one PES-SW-COOH membrane are tested in one day water vapour permeability measurement. WVTR is calculated to be higher in case of PES-SWCOOH membranes. Supposing same diameter of pore size, water permeability can be product of hydrophobic effect inside membrane channels. Carbon nanotubes have an impact on WVTR and further experiments need to be carried out.

D. Molecular Weight Cut Off

The primary basis of solute retention is molecular size. Therefore, in general, the retention of a solute is proportional to its molar mass. Most UF membranes are described by their nominal molecular weight cut-off (MWCO), which is usually defined as the smallest molecular weight species for which the membrane has more than 90% rejection (27).

In UP150 PES/PET membrane brochure, MWCO is given 150.000Da and wastewater model solutions varied from 164-991Da molecular weights. Ideal target is considered to create a nanofiltration membrane with MWCO threshold 100-1000Da (28).

The MWCO of a membrane can be determined from the permeation of dilute solutions containing uncharged solutes. Non-ionized Polyethylene glycols (PEG) are usually chosen to characterize a membrane (27). They are water soluble and can be readily obtained with narrow molecular weight distributions. Although there is a certain accumulation of solute at the membrane surface, the use of low feed concentrations eg. 0.03% PEG (3 mg/L in water),

assures that the solute accumulation is not high enough for consideration of gelation or osmotic contributions. For these low concentrations, viscosity and density can be taken as substantially equal to the pure water values. Concentration polarization factor is neglected.

A PEG solution is prepared with several molecular weights in water. In details, 3gr of PEGS with 200.000Da, 100.000Da, 35.000Da, 10.000Da are soluted in 1L deionized water (0.03% PEG). Mixture is ultrafiltrated in operating pressure 2barsultrafiltration unit in laboratory by PES, PES-SWCOOH and PES-Thin COO^- membrane prepared by spin coating method. Results are gathered below. Filtrated solution is characterized in Gel Permeation Chromatography (GPC) unit. As assumed, the PEG did not foul the membrane extensively because the PEG is non-ionized and it has a low solute membrane surface interaction.

Gel Permeation Chromatography (GPC) is a chromatographic technique that separates dissolved molecules on the basis of their size by pumping them through specialized columns containing a microporous packing material. As the sample is separated and eluted from the column, it can be characterized by a single concentration detector (Conventional Calibration) or series of detectors (Universal Calibration and Triple Detection) (29).

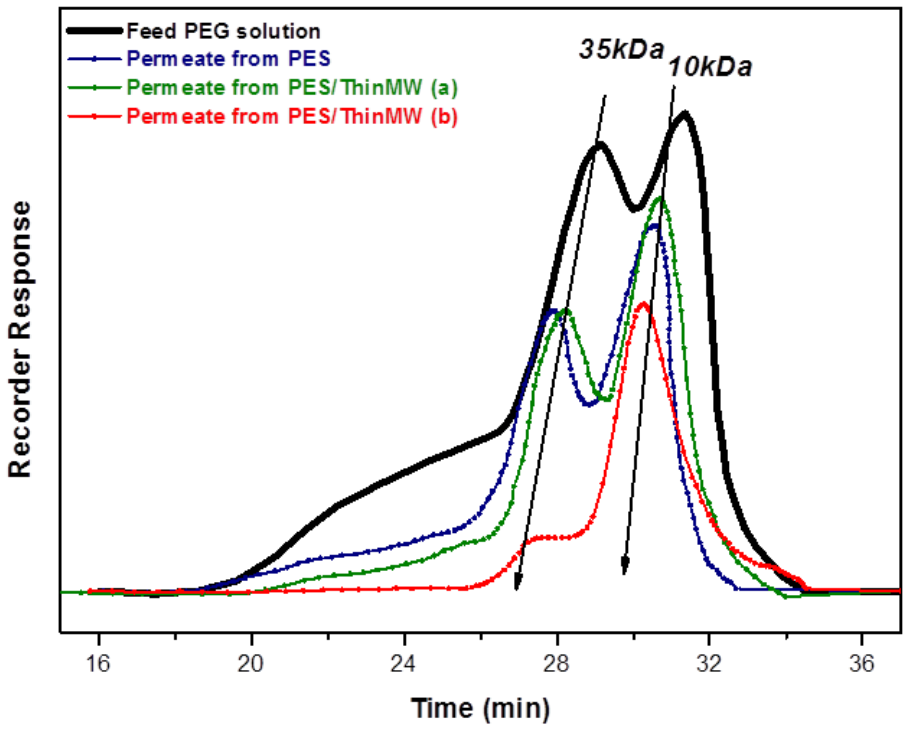

Figure 33 GPC results for molecular weight cut off value of mixed matrix PES-CNTs membranes using 200, 100, 35 and 10 kDa

Three different membranes have been picked up by laboratory made PES membranes and tested in GPC apparatus. The results show an overall promising retention of high molecular weights and even the sample cannot be totally representative a clear tendance is illustrated (Figure 33). The retention of high MW PEGs is close to 100% for PES/Thin MW CNTs membranes (sample (a) and (b)). Sample (b) has a significant cut off on 35kDa. One only value cannon express retention it can though contribute to plan new experiments for further study.

5.7 Conclusions of Part B

Measurements results report the performance of mixed matrix and asymmetric polyethersulfone ultrafiltration flat sheet membranes with carbon nanotubes. Three different types of membranes are prepared. Pure PES membranes, PES blended with SWCNTs membranes and PES blended with Thin MW-COO^- membranes. The membranes are prepared by phase inversion process containing polyethersulfone (PES) as polymer (10% wt., N,N-dimethylformamide (DMF) as solvent of polymer, SWCNTs in N-Methyl-2-pyrrolidone (NMP) as a solvent (0.5%wt. respect to polymer) or Thin MW-COO^- CNTs in NMP (0.5%wt. respect to polymer).

Blend membranes displayed a higher flux and slower fouling rate than the PES membranes. Subsequent analyses of the desorbed foulants showed that the amount of foulant on bare PES membranes was higher than the blend membrane for 0.5% SWCNTs content. Thus, the carbon nanotube content of membranes is shown to alleviate the membrane fouling caused by natural water.

SWCNTs show also far higher water permeability than Thin MW-COO^- incorporated in PES membrane and in all the cases mixed matrix membranes had better efficiency than pure PES membrane.

As the method can considered as comparatively easy and low cost, further study is needed to optimized the different amount of components and evaluate the scale up possibility.

Literature

(1) D. Zagklis, P. Koutsoukos, C. Paraskeva, A Combined Coagulation/Flocculation and Membrane Filtration Process for the Treatment of Paint Industry Wastewaters, Ind. Eng. Chem. Res., 51, 15456−15462 (2012).

(2) T. Deblonde, C. Cossu-Leguille, P. Hartemann, Emerging pollutants in wastewater: A review of the literature, Journal of Hygiene and Environmental Health, 214, 442−448 (2011).

(3) A.Y. Zahrim, C. Tizaoui, N. Hilal, Coagulation with polymers for nanofiltration pre-treatment of highly concentrated dyes: A review, Desalination, 266, 1–16 (2011)

(4) N. Tzoupanou, Preparation, properties and applications of innovative aluminum reagents for coagulation for water purification and wastewater treatment, PhD Thesis, Aristotle University of Thessaloniki, Greece (2009).

(5) M.A. Aboulhassan, S. Souabi, A. Yaacoubi, M. Baudu, Improvement of paint effluents coagulation using natural and synthetic coagulant aids. Journal of Hazardous Materials, 138, 40−45 (2006).

(6) M. Hammer, Water and Wastewater Technology, Wiley, New York, United States (1986).

(7) B. Durham, M. Bourbigot, T. Pankratz, Membranes as pretreatment to desalination in wastewater reuse: operating experience in the municipal and industrial sectors, Desalination, 138, 83−90 (2001).

(8) T. Ratto, J. Holt, A. Szmodis, Asymmetric Nanotube Containing Membranes, U.S. Patent 20110290730 (2011).

(9) T. K. Karachalios, S. F. Nitodas, Influencing factors towards a scalable synthesis of aligned carbon nanotubes by chemical vapor deposition, ECS Transactions 25, 749-756 (2009).

(10) J. Anastasopoulos, BioNexGen Report, University of Patras, Greece (2013).

(11) O.Bkajin, A.Noy, F.Fornasiero, H.G. Park, S.Kim, Membranes with functionalized carbon nanotube pores for selective transport, U.S. Patent 20110253630, issued in November 2011, (2011).

(12) A. Noy, H. G. Park, F. Fornasiero, J.K. Holt, C. P. Grigoropoulos and O. Bakajin, Nanofluids in CNTs, Nanotoday 2, 22-29 (2007).

(13) V. Upadhyayula, S. Deng, M. Mitchell, G. Smith, Application of carbon nanotube technology for removal of contaminants: A review, Science of Environment 408, 1 (2009).
(14) C. Tang, Q. Zhang, K, Wang, Q. Fu, and C. Zhang, Water transport behavior of chitosan porous membrane containing MWNTs, J. Membr. Sci. 337, 240-247 (2009).
(15) M. Majumder, N. Chopra, B.J. Hinds, Nanoscale Hydrodynamcs: Enhanced flow in carbon nanotubes, Nature 438, 44 (2005).
(16) B. Corry, Designing Carbon Nanotube Membranes for Efficient Water Desalination, J. Phys. Chem. B 112, 1427-1434 (2008).
(17) J. Holt, H. Park, Y. Wang, M. Stadermann, A. Artyukhin, C. Grigoropolous, A. Noy, O. Bakajin, Fast mass transport through sub-2-nanometer carbon nanotubes, Science 312, 1034-103 (2006).
(18) M. Majumder, N. Chopra, B.J. Hinds, Effect of tip functionalization on transport through vertically oriented carbon nanotube membranes, J. Am. Chem. Soc. 127, 9062-9070 (2005).
(19) A. Alexiadis and S. Kassinos, Molecular Simulation of Water in Carbon Nanotubes, Chem. Rev. 108, 5014-5034 (2008).
(20) S.Kar, R.C. Bindal, P.K. Tewari, Carbon nanotube membranes for desalination and water purification: Challenges and opportunities Nano Today 7, 385 (2012).
(21) G.Voyiatzis, Sonication workshop presentation, University of Patras, Greece (2010).
(22) http://www.millipore.com/catalogue/item/vvlp04700 (2013).
(23) R.Fries, S.Gebler, M.Simko, Carbon nanotubes – Part II: Risks and Regulations, Nanodossier 24, 1 (2012).
(24) J.Yu, N.Grossiord, C.Konin, J.Loos, Controlling the dispersion of multi-wall carbon nanotubes in aqua surfactant solution, Carbon 45, Issue 3, 618-623 (2007).
(25) E.Celik, H.Park, H.Choi, H.Choi, Carbon nanotube blended polyethersulfone membranes for fouling control in water treatment, Water Research 45, 274-282 (2011).
(26) E.Moschopoulou, Water Vapor Permeability, University of Patras, Greece (2013).
(27) N.Hilal, M. Al-A bri, H. Al-Hinai, Characterization and retention of UF membranes using PEGs, Desalination 206, 568-578 (2007).
(28) D.Sklavounaki, Embeddement of porous polymeric membranes with carbon nanotubes, Master Thesis, University of Patras, Greece (2012).
(29) http://www.malvern.com/labeng/technology/gel_permeation_chromatography_theory/gpc_sec_theory.html (2013).